NPL
National Physical Laboratory

NPL REPORT AC 27

CHARACTERISATION OF ACOUSTIC FIELDS GENERATED BY EXPLOSIVES - QUARRY TRIAL OF APPLICATION OF NOISE ABATEMENT TECHNOLOGY

FREYA MALCHER, PAUL LEPPER

NOVEMBER 2025

Characterisation of acoustic fields generated by explosives - Quarry trial of application of noise abatement technology.

(DESNZ Offshore Energy SEA Sub-Contract OESEA-24-164)

Freya Malcher
Ultrasound and Underwater Acoustics Group

Paul Lepper
Loughborough University

ABSTRACT

This report describes the work undertaken in the project *"Characterisation of acoustic fields generated by explosives - Quarry trial of application of noise abatement technology."*. The aim was to investigate the effectiveness of bubble curtains used as a barrier mitigation for the acoustic output from explosive sources by conducting controlled experimental trials in a quarry facility. This work was funded by the UK Government's Department for Energy Security & Net Zero (DESNZ) through the Offshore Energy Strategic Environmental Assessment programme (OESEA), Sub-Contract OESEA-24-164.

A total of twenty-three explosive tests were undertaken during a six-day trial at the Limehillock Quarry test facility in order to assess how different properties of the bubble curtain affect the attenuation of the acoustic signal generated by underwater explosions. Three different test regimes were conducted to see how the attenuation provided by the bubble curtain changed: the charge size, the distance between the curtain and the charge and parameters of the bubble curtain (flow rate and number of curtain layers).

The results showed that an increase in the charge size showed a reduction in the attenuation observed. That increasing the distance between the curtain and the charge increases the attenuation provided by the curtain up to around 3x the explosive bubble radius. And lastly, that varying the parameters of the bubble curtain flow rate have an impact on the attenuation provided.

ISSN: 1754-2936

https://doi.org/10.47120/npl.AC27

National Physical Laboratory
Hampton Road, Teddington, Middlesex, TW11 0LW

Approved on behalf of NPLML by
Srinath Rajagopal, Science Area Leader.

CONTENTS

EXECUTIVE SUMMARY

1 INTRODUCTION 1

1.1 BACKGROUND 1

1.2 SCOPE OF WORK 2

2 EXPERIMENTAL METHODOLOGY 2

2.1 TEST FACILITY – LIMEHILLOCK QUARRY, SCOTLAND 2

2.2 MEASUREMENT CONFIGURATION 3

2.2.1 Sound pressure measurement 4

2.2.2 Bubble curtain measurements 6

2.2.3 Preparation of explosive sources 7

2.3 BUBBLE CURTAIN OPERATION 10

3 RESULTS 12

3.1 TIME DOMAIN WAVEFORMS 12

3.2 TEST A - CHARGE SIZE 15

3.3 TEST B – STAND-OFF FROM CURTAIN 16

3.4 TEST C – VARYING CURTAIN PARAMETERS 17

3.5 OPTICAL & BUBBLE CURTAIN DATA 19

4 CONCLUSION 21

4.1 SUMMARY 21

4.2 DISCUSSION 21

4.3 FUTURE WORK 21

1 INTRODUCTION

1.1 BACKGROUND

The location and spatial size of many offshore wind farm developments and cable connector projects means there is a high potential to encounter unexploded ordnance (UXO) during construction. This is particularly so in the southern North Sea and Irish Sea due to overlap with World War I and World War II conflict areas, military training areas and munitions disposal sites, but it is also relevant in Scottish waters. As part of development planning, detailed surveys are undertaken to identify possible UXO and confirm what action is needed to reduce health and safety risks to a tolerable level. When UXO cannot be avoided or safely removed, detonation on site (BiP Blast-in-Place) may be necessary (subject to obtaining required licences). A good understanding of the number and type/size of detonations carried out each year across the UK Continental Shelf (UKCS) especially for wind farm developments, would be a valuable resource, particularly if the levels of acoustic noise radiated were recorded. At present, there is no single complete record of such detonations in UK waters.

A common methodology used for the disposal of these UXO is the deliberate detonation in-situ initiated by a small (typically 5-10 kg TNT equivalent) donor charge placed on the munition to initiate an explosive detonation of both the donor and the main charge. These ‘high-order’ events can produce significant acoustic levels in the water column and the seabed (Robinson et al., 2022). These events can produce some of the highest sound pressures of all anthropogenic sound sources with the potential to cause fatal injury to marine mammals and other marine fauna in close proximity to the blast, but also auditory damage and behavioural responses at much longer ranges.

The JNCC guidelines (JNCC, 2010) focus on minimising the risk of physical trauma and permanent auditory injury (PTS). The distance at which detonations could cause physical injury must be established as part of a noise risk assessment to inform the licensing process and estimate the effectiveness of mitigation measures. The NMFS thresholds (National Marine Fisheries Service, 2018, 2024) incorporate the latest research results and provide an update of the 2007 (Southall et al., 2007) thresholds referred to in the guidelines and have been adopted by Statutory Nature Conservation Bodies (SNCBs). Estimates of PTS injury zones for unmitigated events compared to NMFS thresholds have resulted in much larger impact ranges than were previously estimated, extending in the most extreme cases well beyond any effective mitigation zone (e.g. up to 15 km from detonation for a UXO charge of >700 kg). Such results raise grave concern for the protection of the marine environment and for industry, as the consequence of a risk assessment concluding that an UXO detonation is likely to result in a large PTS injury zone is onerous.

Recent work has shown that the use of alternate ‘low-order’ deflagration technologies (internal combustion initiated using small-shaped charges) can reduce the severity of the impact compared to high-order detonation events through the possibility of lower acoustic source levels and therefore lower impact ranges (Robinson et al., 2020).

In January 2025 a new policy paper was published titled ‘Marine environment: unexploded ordnance clearance Joint Position Statement’ (Department for Environment, Food and Rural Affairs, 2025) highlighting the requirement for low noise methods of clearance and noting that technological development in this area is encouraged.

Bubble curtains offer another potential low-order technology that has been used successfully for mitigation of sound sources such as the marine pile driving (Bohne et al., 2019; Domenico, 1982; Loye & Fred Arndt, 1948; Schmidtke, 2010). Research has shown that bubble curtains can also be used to mitigate explosive sources (Croci et al., 2014; Schmidtke, 2012; Sebastian Bryson et al., 2021). However, these studies give limited insight into how the properties of the

curtain can be adapted to maximise the attenuation or of the differences between effectiveness on impulsive pressure such as piling, and impulsive shock wave sound sources such as detonations. More recent works have started to investigate such topics (Beelen et al., 2024; Dam & Tran, 2021) but there is still extensive research to be done in this area.

1.2 SCOPE OF WORK

The scope of this work is to provide information to inform on the effectiveness of air bubble curtain properties in the reduction of acoustic levels specifically from underwater explosive events in combination with other mitigation strategies such as low-order deflagration. This will help identify appropriate mitigation (singular or combinational), underpin more realistic exposure assessments and guide EPS licence applications/decisions.

Three sets of tests were conducted for this phase of the work. The first test investigated how the attenuation from a bubble curtain is impacted by different charge sizes. The second test investigated how varying the distance between the bubble curtain and the explosion impacts the attenuation. The third test looked at a fixed charge size and varied the bubble distribution of the bubble curtain (through either air flow rate or multiple curtains).

2 EXPERIMENTAL METHODOLOGY

2.1 TEST FACILITY – LIMEHILLOCK QUARRY, SCOTLAND

The test facility is operated by Thornton Tomasetti Defence Ltd, a multidisciplinary company who specialise in structural shock testing using explosives and seismic airgun technology. Their main facility at Limehillock Quarry is a unique inland underwater testing facility licensed for a wide range of test targets and with access suitable for testing of naval structures to UK and NATO standards. Thornton Tomasetti operates a number of Shock Test Vehicles for use in underwater shock testing and their shock barge has an available test deck area of around 8.4 m x 4 m and a weight capacity of approximately 25 tonnes.

The Limehilllock test facility was hired for 5 days to facilitate the testing of the noise abatement technologies, which included Thornton Tomasetti's expertise in explosive shock testing, underwater pressure monitoring services and the use of their equipment onsite. It also provides facilities to carry out all test activities including charge preparation and deploying of additional equipment according to the test requirements.

The quarry has dimensions of approximately 250 m long by 125 m wide, is a little over 20 m deep on average and is filled with fresh water (Figure 1). The bathymetry between the position of the explosive source and that of the furthest hydrophone was 20.1 m ±1 m. During the trial, the water temperature varied from 11°C and 16°C for the shallowest 5 m of the water column, but beneath this depth a thermocline can be observed with the temperature quickly decreased to 4.9 °C at the bottom with a temperature of 6.24°C measured at 8 m (the charge depth).

Figure 1 Limehillock Quarry - hillside viewpoint

2.2 MEASUREMENT CONFIGURATION

In order to characterise the acoustic output from explosion and to evaluate the effect of the bubble curtain, acoustic measurements were recorded at three measurement locations with two near-field measurements and a far-field measurement, all with sensors suspended from the water surface. These were: (i) either side of the bubble curtain (nominally 3 m from the charge before the curtain and 3 m from the charge after the curtain) and (ii) at a distance of 163 m from the bubble curtain (at the far end of the quarry). The near-field sensor was placed inside and outside the bubble screen in order to allow comparison of measurements with/without the presence of bubble screen and reference measurements were taken without a bubble curtain active to allow comparison in the far-field data. The configuration and deployment may be seen in Figure 2.

Thornton Tomasetti provided the instrumentations to measure the near-field response from the explosion which were deployed from shoreside station. NPL and Loughborough University provided the far-field measurement equipment which consisted of a three-element vertical hydrophone array. A sound particle motion sensor with bespoke underwater logger was also deployed to measure the particle motion of the signal from the explosive source (results reported separately). This was deployed from a floating shock test vehicle (STV01) with an undercover area to provide weather protection to the data acquisition system and power supplies.

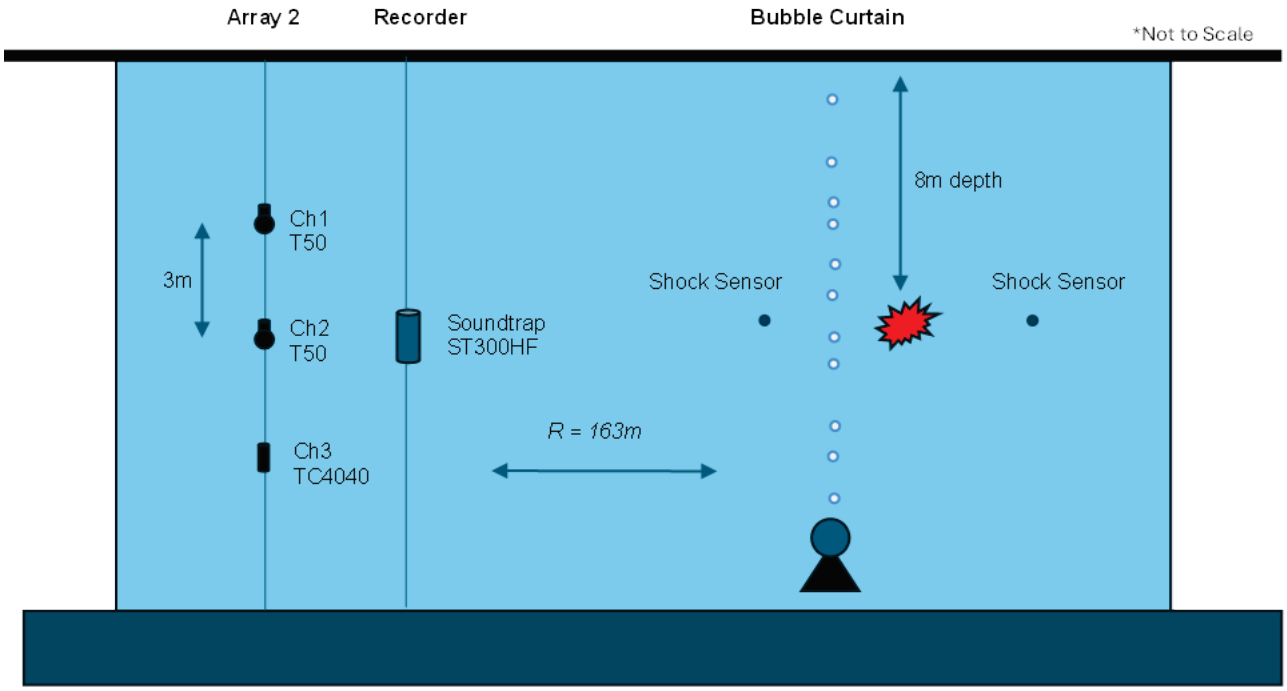

Figure 2 Schematic of the measurement configuration for the near and far field.

2.2.1 Sound pressure measurement

For the nearfield measurements, two types of underwater shock transducers were employed: T11 transducers (manufactured by Neptune Sonar, nominal charge sensitivity: 0.07 pC/kPa; maximum pressure: 275 MPa) and 138A26 transducers (manufactured by PCB, nominal voltage sensitivity: 0.29 µV/Pa; maximum pressure: 172 MPa). The shock transducers were powered by a PCB 482C05 four-channel unity-gain signal conditioner with additional PCB 422E06 charge amplifiers being used for the T11 transducers. A 16-channel 1MHz Yokogawa DL750 data recorder was used for capturing the data. All data were sampled at 500 kilosamples per second giving a time base resolution of 2 µs. Each measurement was recorded for a duration of 5 seconds. The DL750 data acquisition system was triggered by a 'Charge Probe' which is fixed directly to the explosive and provided a voltage step at the time of detonation. The shock pressure sensors were suspended from floating pontoons (Figure 3 4) and due to a minor re-positioning of the source between detonations, their separation distances varied slightly between measurement sets. The distances were measured on the surface with a laser rangefinder (confirmed by the acoustic propagation delay). All four sensors were deployed at 8 m water depth, the same depth chosen for all of the source charges.

For far field measurement, a three-element hydrophone array was deployed from Thornton Tomasetti's shock test vehicle STV01 (Figure 3 and Figure 5a & b). The array consisted of two T50 hydrophones (manufactured by Neptune Sonar, with nominal sensitivity 28 µV/Pa) and one Reson TC 4040 hydrophone. The line array was configured with only low-sensitivity hydrophones to avoid system saturation due to the expected high amplitude pulses generated during the high-order detonations. In addition to these acoustic sensors, a Soundtrap ST300 (manufactured by Ocean Instruments, with high gain nominal sensitivity -186 dB V/µPa) was deployed at mid-water column for the duration of the trial to determine the background noise level. This was also moved close to the curtain for some set up tests to collect the sound from the curtain. The acquisition was made using a PicoScope 4824 sampling at 10 mega-samples per second (time resolution of 0.1 µs) recording for 5 seconds and triggered electronically based on the level prediction of the charge size of the explosive.

NPL and Loughborough University instruments were completely independent and recorded by two different digitisers simultaneously, providing some redundancy in order to avoid data loss by unexpected system failure.

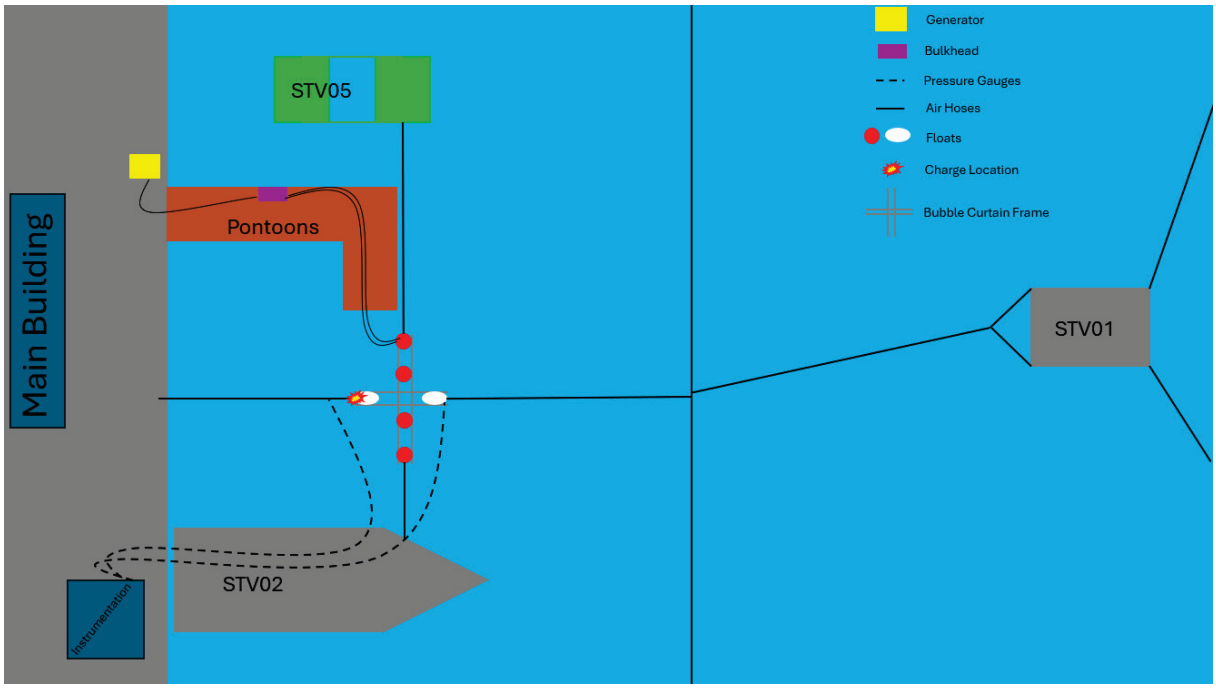

Figure 3 Test configuration of the quarry site.

Figure 4 Photographs of the bubble curtain and far-field instrumentation on the shock test vehicle.

Figure 5 Photographs of the bubble curtain and far-field instrumentation on the shock test vehicle.

The line-array hydrophones were calibrated traceable to national standards in the laboratory before the trial using the methods described in IEC 60565 [IEC 60565 2019 & 2020]. This was done by comparison in a closed coupler in the range 5 Hz to 315 Hz. Free-field reciprocity was used to calibrate the T50 hydrophones over the frequency range 750 Hz to 200 kHz.

2.2.2 Bubble curtain measurements

In order to observe the bubble curtain in operation, camera equipment was deployed in front of the bubble curtain, on the other side of the curtain to the charge.

A variety of camera equipment was used. For photographs of the bubbles, an Olympus Tough TG-7 camera was used, with overhead flash system & underwater casing. Two Go-Pro 11's with independent underwater backlights were used to take videos of the bubbles. The Soundtrap was also deployed on this rig in order to take sound recordings of the bubbles.

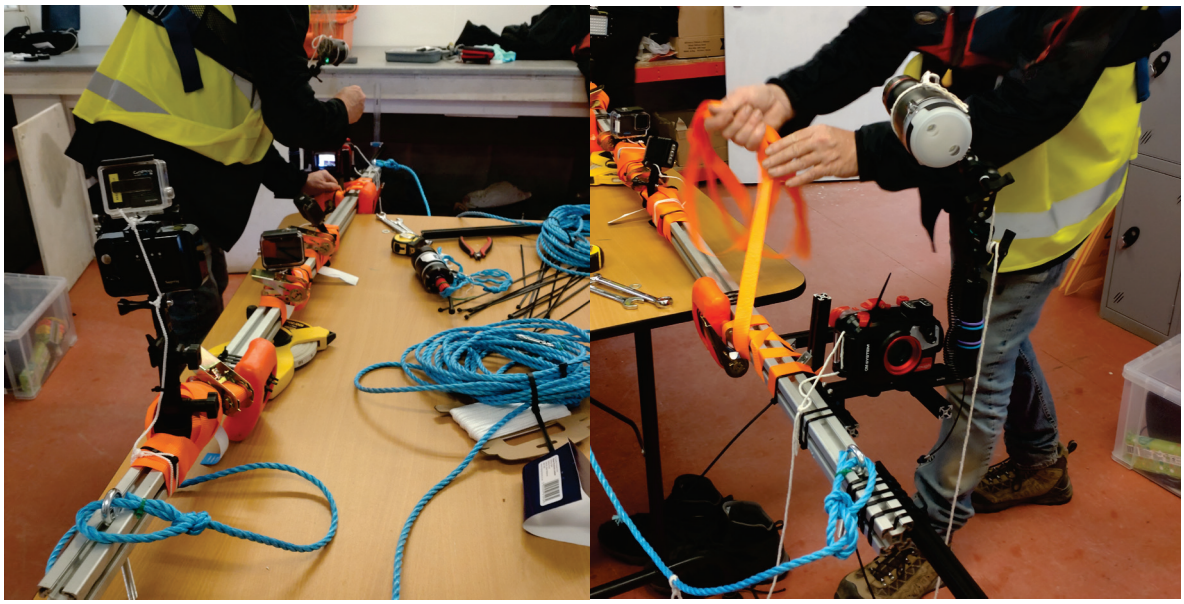

Figure 6 Photographs of the bar used to deploy the camera equipment.

This system was suspended horizontally off two ropes at the charge depth (8 m). The system was deployed to take photographs of the bubble curtain on two occasions; whilst no explosives were taking place (in order to not damage the camera & Soundtrap); then these were removed leaving the GoPros in place whilst the explosions were being carried out. During the two deployments with the camera & Soundtrap, a variety of flow rates were tested for the bubble curtain to observe the bubble size for each set up. The GoPros were left in place during the explosions to investigate if the explosive bubble interacted with the bubble curtain. It was expected that data from the GoPros would be limited as they risked being damaged during the explosion(s). Additional GoPro 11's were deployed to record in-air aspects of the tests at various vantage points.

2.2.3 Preparation of explosive sources

To simplify the test and maximise the usefulness of the data, 23 charges were prepared as follows: 5x 25 g charges, 14x 100 g charges, 2x 250 g charges and 2x 500g charges.

Each test took approximately 30 mins to complete, this is to allow safe deployment, recovery and required inspections pre- and post-test for the detonations. The number of munitions/charges and order of the munitions used was agreed with the operators prior the start of the trial in order to prioritise the more important tests to ensure a comprehensive dataset. All charges were fired using shock tube connected to a detonator. Two charges were only partially detonated (1x 25g and 1x 100g) leaving 21 successful detonations.

The test schedule and associated details are described in Table 1-3 below.

Table 1 Test schedule and details.

Bubble Curtain	**Test 1**	**Test 2**	**Test 3**	**Test 4**	**Test 5**	**Test 6**	**Test 7**
Date	19/05/25	19/05/25	19/05/25	20/05/25	21/05/25	21/05/25	21/05/25
Test Series	AR	AR	AR	AR	A	A	A
Charge Size	25g	100g	250g	500g	25g	100g	250g
Bubble curtain Flow (%)	0	0	0	0	100%	100%	100%
Bubble curtain distance to charge	-	-	-	-	3m	3m	3m
Detonation method	Shock Tube	Shock Tube	Shock Tube	Shock Tube	Shock Tube	Shock Tube	Shock Tube
Charge float to STV01 Aft face	162m	162m	162m	161m	161m	161m	161m
Charge float to PG1 / PG2	3m	3m	3m	3m	3m	3m	3m
Charge float to PG3 / PG4	6m	6m	6m	6m	6m	6m	6m
Water depth at charge	18.4m	18.4m	18.4m	18.4m	18.4m	18.4m	18.4m
Charge depth	8m	8m	8m	8m	8m	8m	8m
Shot time	15:10	15:38	15:58	10:18	11:51	12:13	12:36

Table 2 Test schedule and details.

	Test 8	**Test 9**	**Test 10**	**Test 11**	**Test 12**	**Test 13**	**Test 16**
Date	21/05/25	21/05/25	21/05/25	21/05/25	21/05/25	21/05/25	22/05/25
Test Series	A	B	B	B	B	B	C
Charge Size	500g	100g	100g	100g	100g	100g	25g
Bubble Curtain Flow (%)	100%	100%	100%	100%	100%	100%	100% x2
Bubble curtain distance to charge	3m	1.8m	0.3m	1.2m	0.9m	0.6m	3m

Detonation method	Shock Tube	Shock Tube	Shock Tube	Shock Tube	Shock Tube	Shock Tube	Shock Tube
Charge float to STV01 Aft face	161m	161m	161m	161m	161m	161m	162m
Charge float to PG1 / PG2	3m	4.2m	5.7m	4.8m	5.1m	5.4m	3m
Charge float to PG3 / PG4	6m	4.8m	3.3m	4.2m	4.9m	4.6m	6m
Water depth at charge	18.4m	18.4m	18.4m	18.4m	18.4m	18.4m	18.4m
Charge depth	8m	8m	8m	8m	8m	8m	8m
Shot time	13:03	14:44	15:06	15:28	15:46	15:59	12:31

Table 3 Test schedule and details.

	Test 17	**Test 18**	**Test 19**	**Test 20**	**Test 21**	**Test 22**	**Test 23**
Date	22/05/25	22/05/25	22/05/25	22/05/25	23/05/25	23/05/25	23/05/25
Test Series	C	C	C	C	C	C	C
Charge Size	100g	100g	100g	100g	25g	100g	100g
Bubble Curtain Flow (%)	100% x2	60%	50%	40%	60%	60%	60%
Bubble curtain distance to charge	3m	3m	3m	3m	3m	3m	3m
Detonation method	Shock Tube	Shock Tube	Shock Tube	Shock Tube	Shock Tube	Shock Tube	Shock Tube
Charge float to STV01 Aft face	162m	162m	162m	162m	160m	160m	160m
Charge float to PG1 / PG2	3m	3m	3m	3m	3m	3m	3m
Charge float to PG3 / PG4	6m	6m	6m	6m	6m	6m	6m
Water depth at charge	18.4m	18.4m	18.4m	18.4m	18.4m	18.4m	18.4m
Charge depth	8m	8m	8m	8m	8m	8m	8m
Shot time	14:51	15:19	15:34	15:49	10:34	10:55	11:17

2.3 BUBBLE CURTAIN OPERATION

The basic principle of bubble curtain involves the creation of a barrier of bubbles in the water column from the quarry floor to the water surface using a large air compressor. The system uses a perforated hose or pipe, which releases compressed air into the water to form the curtain of bubbles. Two different bubble curtains were tested (BUB1.0 and BUB1.25), the details for each of the curtains in Figure 6 and Table 2. Two 15 m lengths separated by 20 cm of parallel running bubble curtain hose were attached to a horizontally deployed frame (fig 7) at a depth of 9 m. Each length of bubble curtain hose was individually connected via around 30 m of reinforced weighted 'Torpedo tube' hose directly attached to individual manifold controls as shown in Figure 8. This allowed gas flow control to each hose individually, allowing individual gas flow variation and both single and double curtain deployments. (see Figure 8). The flow rate (per metre of curtain) was varied between 38.3 L/min/m and 83.3 L/min/m throughout the testing. The flow rates tested were guided by those recommended by the curtain manufacturer. The hose systems and the associated equipment for both the types BUB1.0 and BUB1.25 bubble curtains tested were supplied by Frog Environmental Ltd (UK), manufactured by http://Canadianpond.ca.

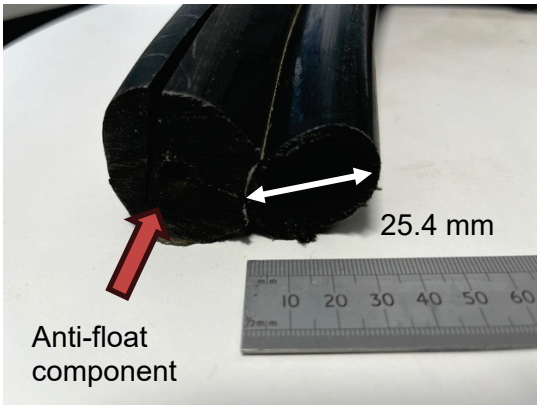

Fig 6.a) 'Small Bubble' (BUB1.0) hose cross section. Hose average inner diameter 25.4 mm

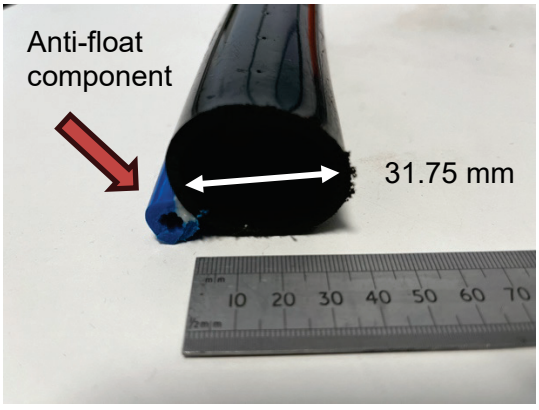

Fig 6.b) 'Big Bubble' (BUB1.25) hose cross section. Hose average inner diameter 31.75 mm

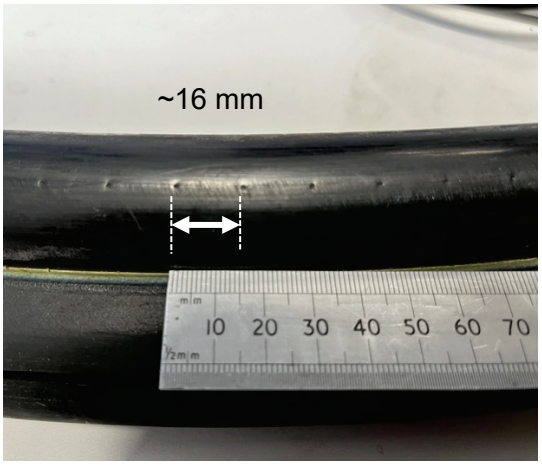

Fig 6.c) 'Small Bubble' 2 x rows of holes ~16 mm spacing

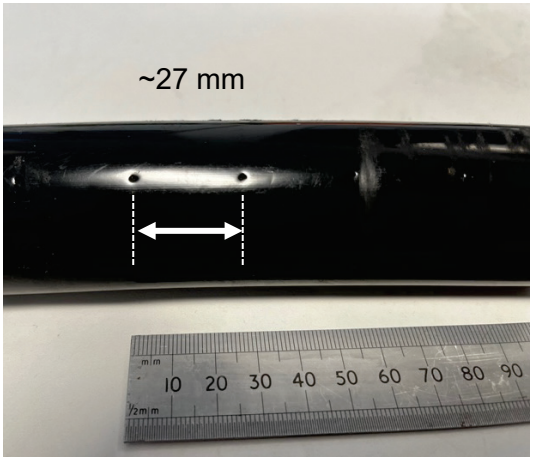

Fig 6.d) 'Big Bubble' 2 x rows of holes, ~27 mm spacing

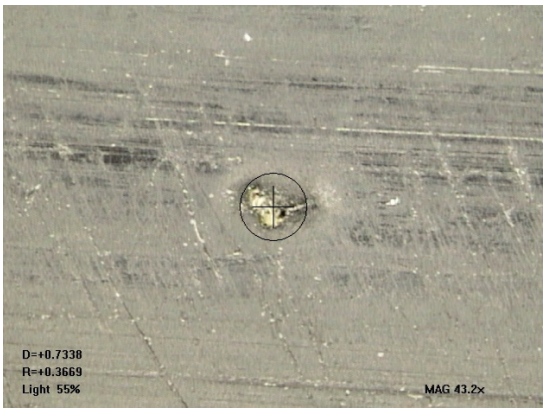

Fig 6.e) 'Small Bubble' (BUB1.0) approximate hole diameter 0.73 mm

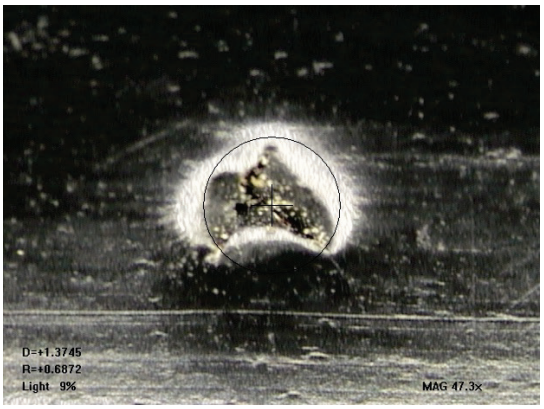

Fig 6.f) 'Big Bubble' (BUB1.25) approximate hole diameter 1.37 mm

Table 2 Curtain parameters

	Small bubble	Big bubble
Manufacture ID	BUB1.0	BUB1.25
Hose diameter	25.4 mm	31.75 mm
Manufactures quoted bubble size	1-10 mm	10-30 mm
Hole spacing	16 mm	27 mm
Hole size estimate	0.73 mm	1.37 mm
No. of rows of holes	x 2	x 2

Figure 7 Photograph of the bubble curtains attached to the frame.

Figure 8 Manifold system for controlling the flow rate of the bubble curtains.

3 RESULTS

3.1 TIME DOMAIN WAVEFORMS

The panel in Figure 9 shows the initial arrival of the pressure wave signal seen on a nearfield T11 sensor at a horizontal range of 6 m for both the 25 g and 100g both with the bubble curtain on and off (reference). The upper panels show a clear positive arrival peak that can be seen at around 4ms indicative of the direct path propagating pressure wave for the 25g and 100g charge sizes of around 1.2 MPa (zero-peak) and 2.6 MPa (zero-peak) respectively. These values correspond well with typical free-field charges of this size (Arons, 1954; Weston, 1960). In the lower two panels the equivalent signal is shown having travelled through the bubble curtain with a flow rate / metre of 67 L/min/m. These show a clear sound reduction which equates to around 10-12 dB for this initial signal size. The ‘with-bubble-curtain’ results also show some variation in the direct path signal structure as well as evidence of generation of some higher frequency components not seen in the without case. These components may be due to non-linear interaction of the acoustic signal and the bubbles.

A lower amplitude secondary negative going transient spike can also be seen at around 11.5 ms (Figure 9) most likely due to surface reflections when the bubble curtain is off. This signal is barely detectable in on cases where the bubble curtain is on, mostly likely due to additional interaction with the bubble curtain in the upper half of the water column. All four cases also show another positive transient signal around 13-14 ms potential from reflections from the walls or bottom of the quarry, which are largely unaffected by the bubble curtain as the signal by-passes the curtain on these propagation paths.

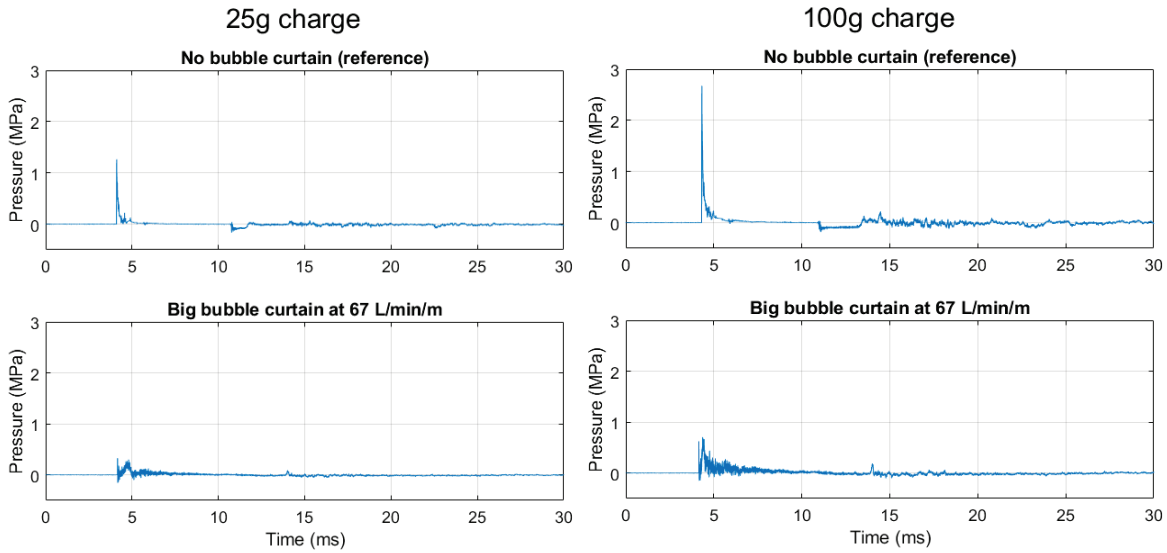

Figure 9 Time domain data for PG3 Thornton Tomasetti pressure gauge in the near field of the explosion (6 m) for two charge sizes.

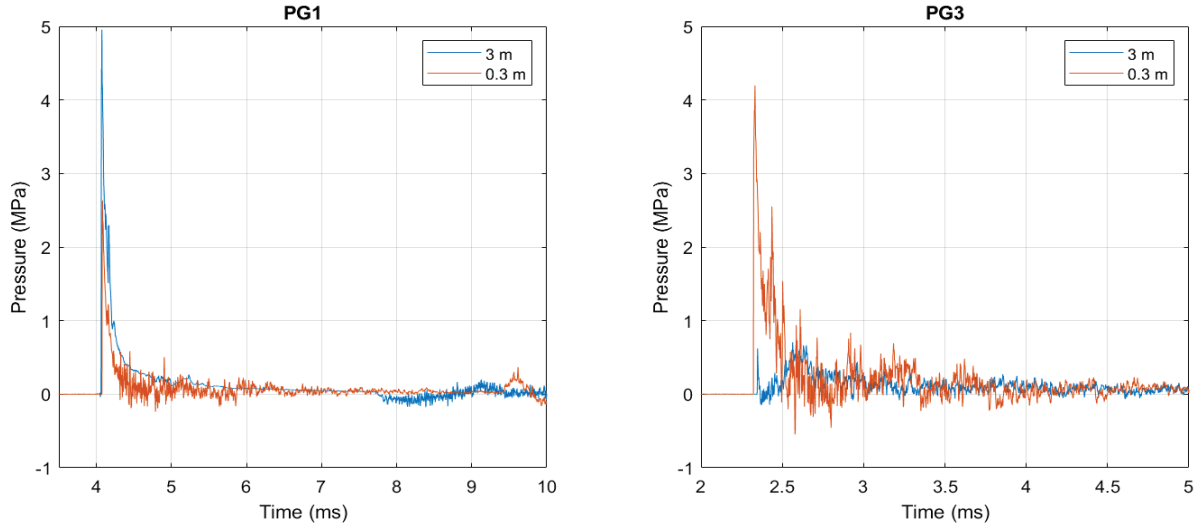

Figure 10 shows near field data for sensors inside (PG1) and outside (PG3) the bubble curtain at two different charge distances away from the curtain. For 0.3 m charge distance PG1 is 5.7m away from the curtain and for 3 m charge distance it is 6m. PG3 is 3m away from the curtain.

It can be seen from Figure 10 that for sensor PG1 at 3m away from the charge, noise is apparent in the signal from ~7.8 ms, 3.8 ms after the initial pulse. This corresponds to time taken for the sound to reach the bubble curtain and reflect back to the sensor. Similar timings are apparent when the sensor is at 0.3 m where this reflection is approximately 0.4 ms after the initial pulse. This highlights that the noise on the signal when the bubble curtain is on is from reflected sound from the bubble curtain itself. For sensor PG3, it can be seen that the bubble curtain noise comes in very quickly after the initial pulse. This could be re-radiation from the bubbles when they interact with the shock wave as it passes through the field, at different angles across the length of the curtain. In the case when the bubble curtain is 3m away from the charge, the peak of this noise can be as loud as the initial pulse. This will be discussed further in Section 3.3.

An example of the time domain waveforms in the far-field is shown in Figure 11. The hydrophone was at the charge depth, approximately 163 m away from the explosion.

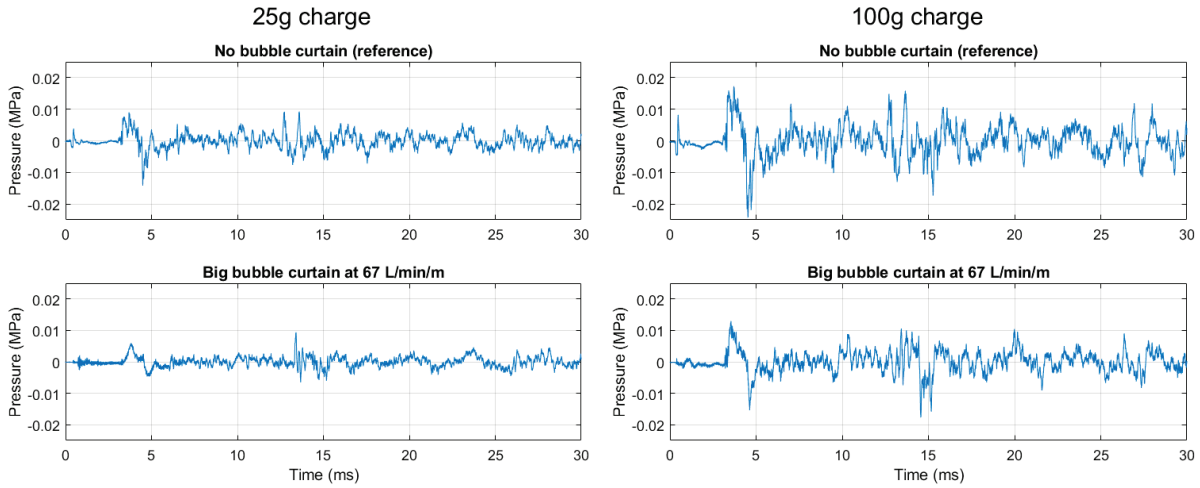

Figure 11 Time domain data for a Neptune T50 hydrophone at 8m depth (in line with the charge) in the far field of the explosion (163 m) for two charge sizes.

It can be seen from Figure 11 that when the bubble curtain is off (reference measurement) there is an initial pulse at low amplitude approximately 0.5 ms (3.0 ms before the main pulse). It is theorised that this pulse is a result of an alternate propagation path for example the walls or bottom of the quarry at a higher sound velocity than the water pathways. This pre-signal is not seen at the near-field shorter ranges The primary propagation (direct) path through the bubble curtain is at approximately 3.5 ms. For both charge sizes shown, a purely visual inspection of the waveform shows that the amplitude of this peak still has been reduced by the presence of the bubble curtain.

3.2 TEST A - CHARGE SIZE

The aim of Test A was to investigate how the attenuation from the bubble curtain would be affected by the charge size. Four charge sizes were tested from 25 g to 500 g. The attenuation was calculated for the near field data based on the ratio of the peak sound pressure level of the pulse inside and outside the curtain. Since the pressure gauge outside the curtain was further away from the charge than the gauge inside, the sound level was corrected assuming spherical spreading. For this test, the big bubble curtain was used at a flow rate of 67 L/min/m.

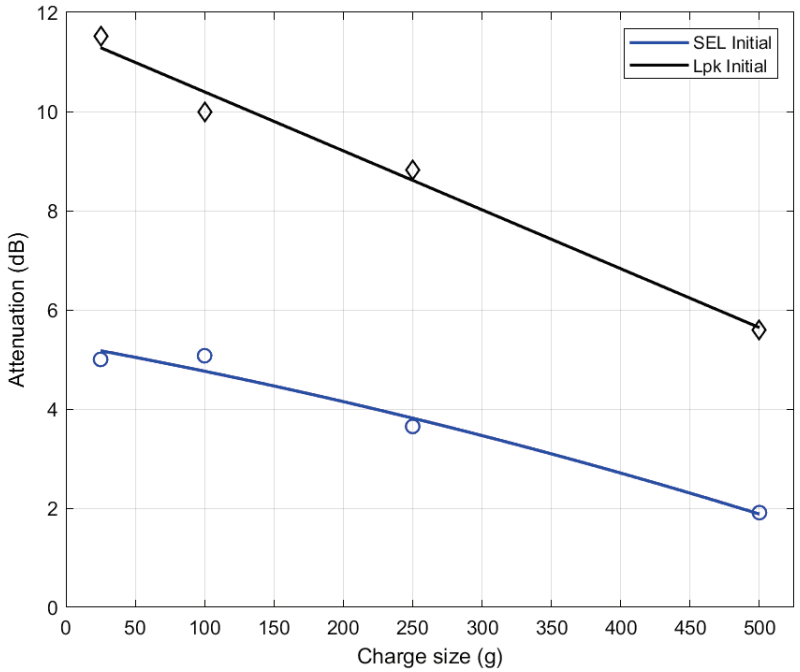

Figure 12 The attenuation provided by the big bubble curtain in terms of peak sound pressure level (L_{pk}) and sound exposure level (SEL) at a flow rate of 67 L/min/m for different charge sizes, calculated using the near field data. [SEL integration window 5 ms, data shown is for the free-field initial signal only.]

It can be seen from Figure 12 that as the charge size increases, the attenuation provided by the bubble curtain reduces. In Figure 13 the attenuation from the sound pressure level is shown with respect to frequency for each of the charge sizes.

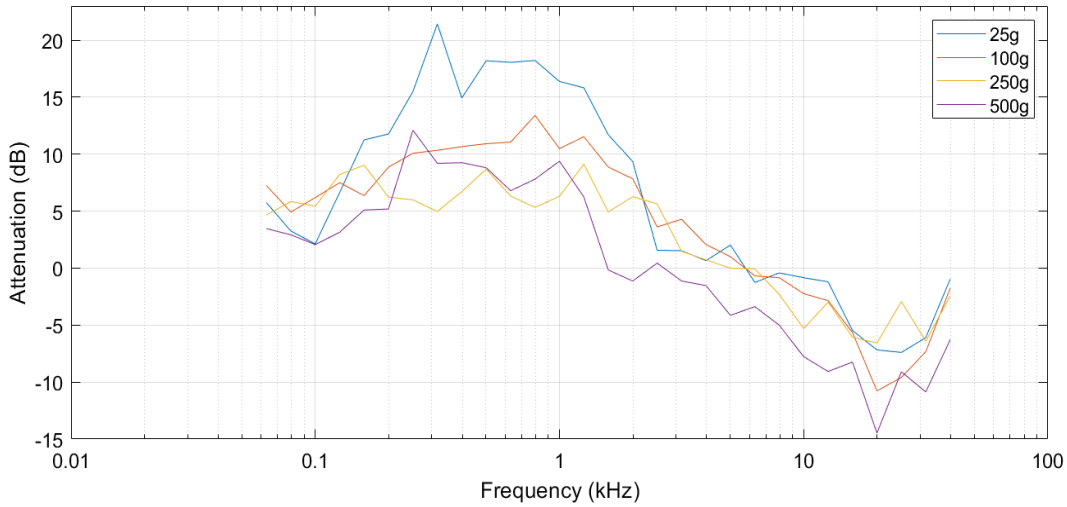

Figure 13 The attenuation with respect to frequency given by the bubble curtain for different charge sizes, calculated using the initial sound field.

3.3 TEST B – STAND-OFF FROM CURTAIN

The aim of Test B was to investigate how the distance from the charge to the bubble curtain (the stand-off distance) would affect the attenuation provided. Six different stand-off distances were tested. The distances were chosen to be multiples of the explosive bubble radius (at 100 g (*W*) and 8 m charge (*H*) depth this is calculated to be 0.6 m using the equation below (Urick, R.J. 1983)

$$3.3825 \cdot \sqrt[3]{\left(\frac{W}{H+10.33}\right)}.$$

The smallest distance was chosen to be 0.3 m so that the explosive bubble would interact with the curtain and the largest was 3 m as to be very far away from the curtain. It should be mentioned here that all other tests in this project used a stand-off distance of 3 m.

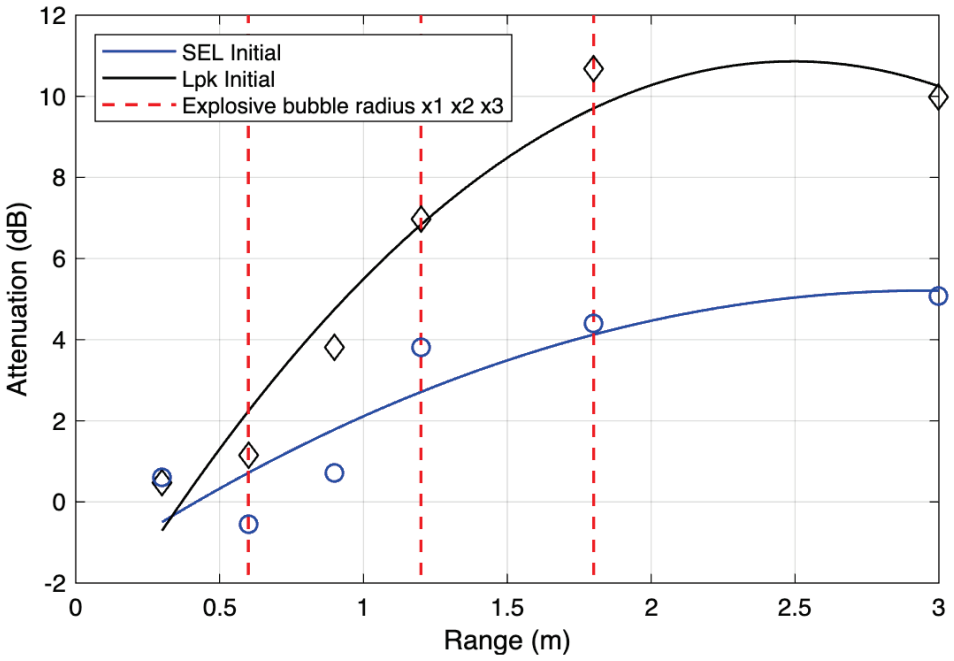

Figure 14 The attenuation provided by the bubble curtain in terms of peak sound pressure level (L_{pk}) and sound exposure level (SEL) for different charge stand-off distances (range), calculated using the near field data. [SEL integration window 5 ms, data shown is for the free-field initial signal only.]

It can be seen from Figure 14 the attenuation appears to plateau as the distance from the curtain increases, particularly from 3x the explosive bubble radius.

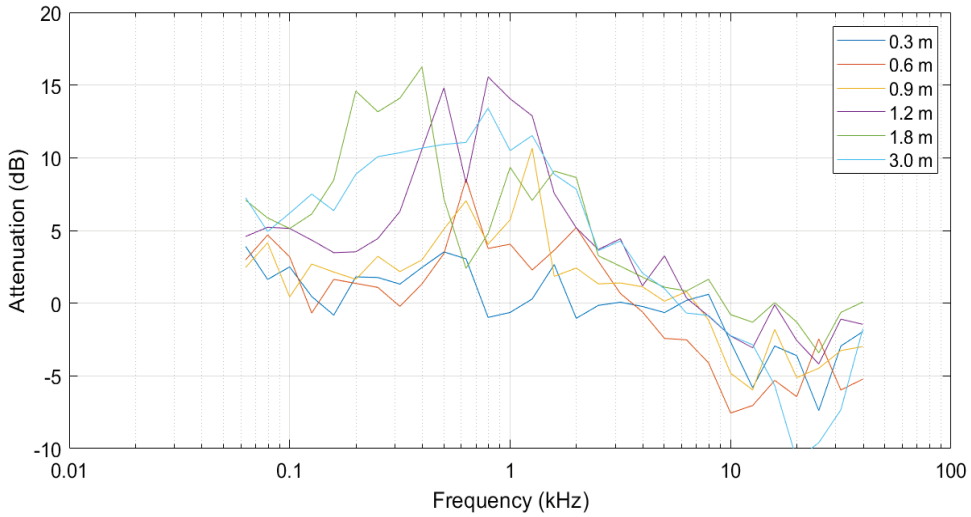

Figure 15 The attenuation with respect to frequency given by the bubble curtain for different charge stand-offs, calculated using the initial sound field.

It can be seen from Figure 15 that the attenuation profile at 1.2 m stand-off and above shows a higher attenuation in the mid frequency region from 1 to 10kHz, and perhaps at a lesser degree between 0.1 - 1kHz. At frequencies other than these ranges the attenuation provided by the bubble curtain is similar.

3.4 TEST C – VARYING CURTAIN PARAMETERS

The last test involved changing some of the flow rate of the curtain to see how these would affect the attenuation provided. The specifications of the curtains used are given in Table 2. Figure 16 shows the attenuation with respect to flow rate for a single layer of the big bubble curtain. This plot is for a 100g charge size.

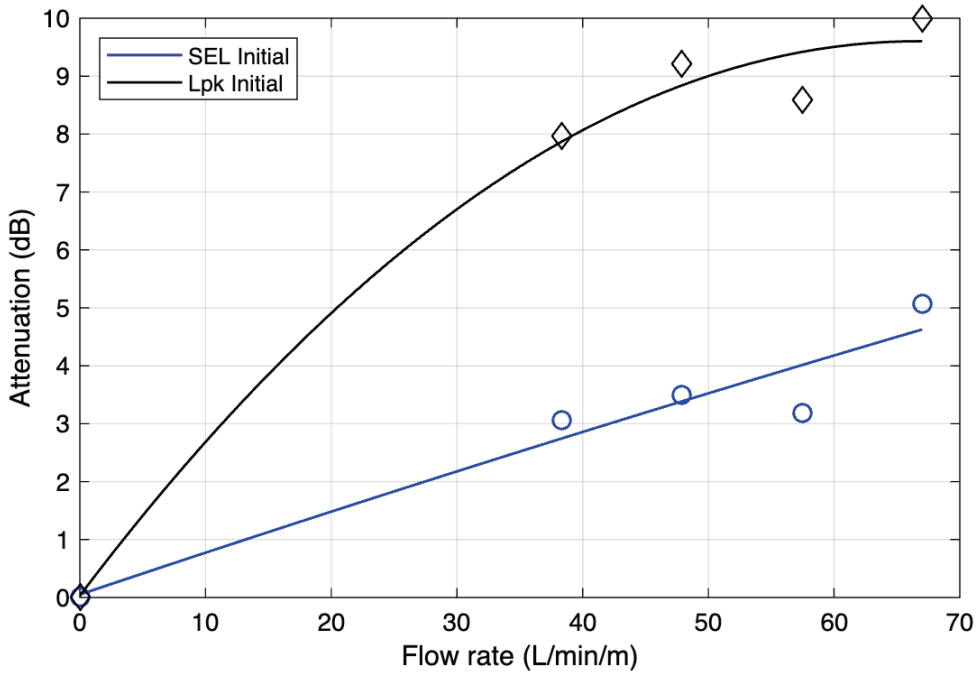

Figure 16 The attenuation provided by the big bubble curtain in terms of peak sound pressure level (L_{pk}) and sound exposure level (SEL) at flow rates between 38 and 67 L/min/m, calculated using the near field data. [SEL integration window 5 ms, data shown is for the free-field initial signal only.]

It can be seen from Figure 16 that the attenuation appears to level off with increasing flow rate when using the peak sound pressure level but shows a more linear trend for the sound exposure level.

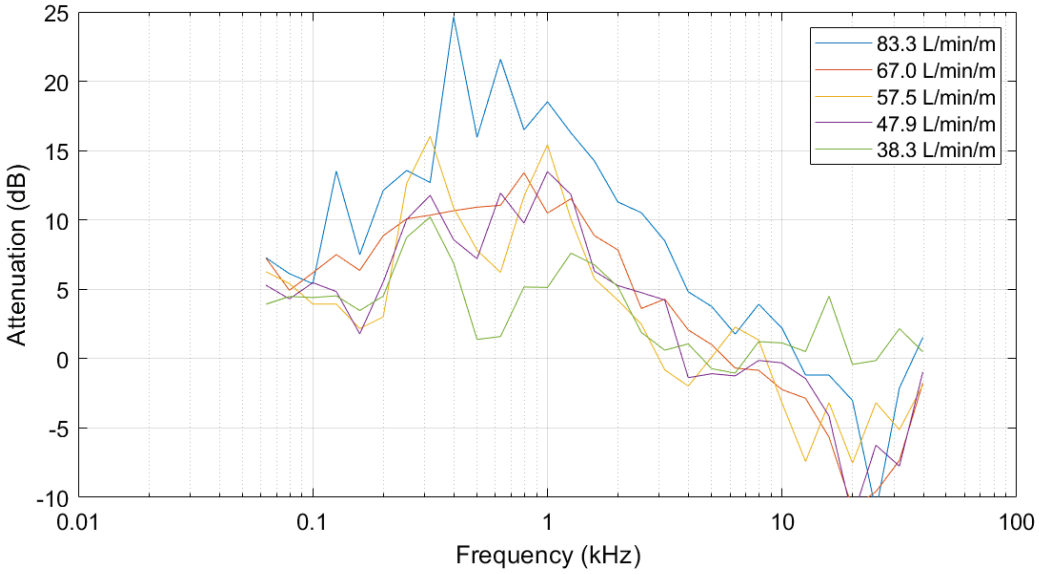

Figure 17 The attenuation with respect to frequency given by the bubble curtain for different flow rates, calculated using the direct sound field.

It can be seen from Figure 17 that the attenuation is higher at the highest flow rate, particularly in the 0.1-1 kHz range, reducing with lower flow rates.

3.5 OPTICAL & BUBBLE CURTAIN DATA

Figure 18 and Figure 19 show examples of the frequency domain signal from the bubble curtain compared to the background noise. Figure 20 show an image taken with the camera of the bubble field.

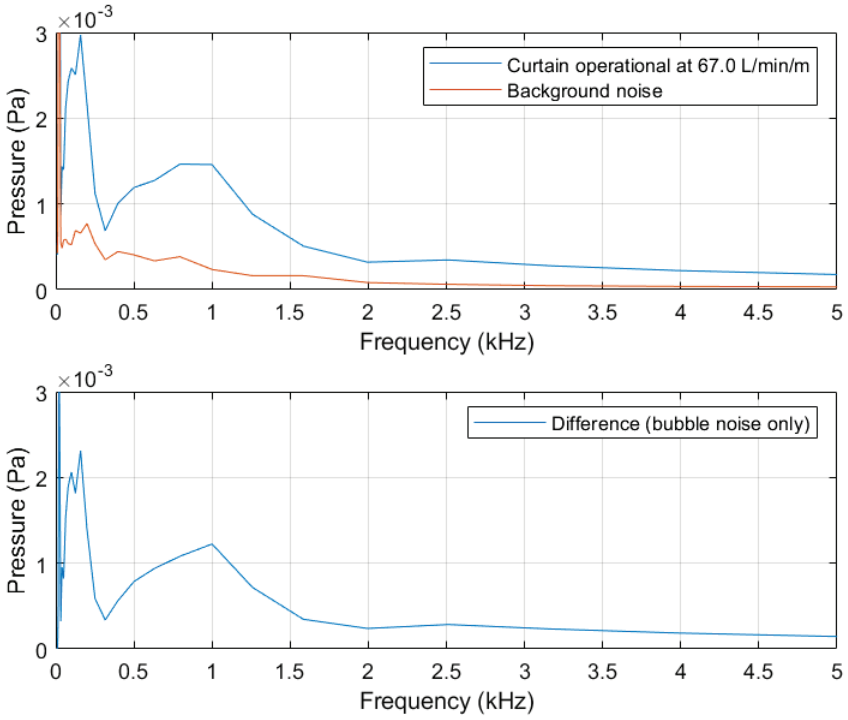

Figure 18 Sound recorded by the SoundTrap for a bubble curtain flow rate of 67.0 L/min/m compared to the background noise level. The SoundTrap was positioned approximately 60 cm away from the curtain.

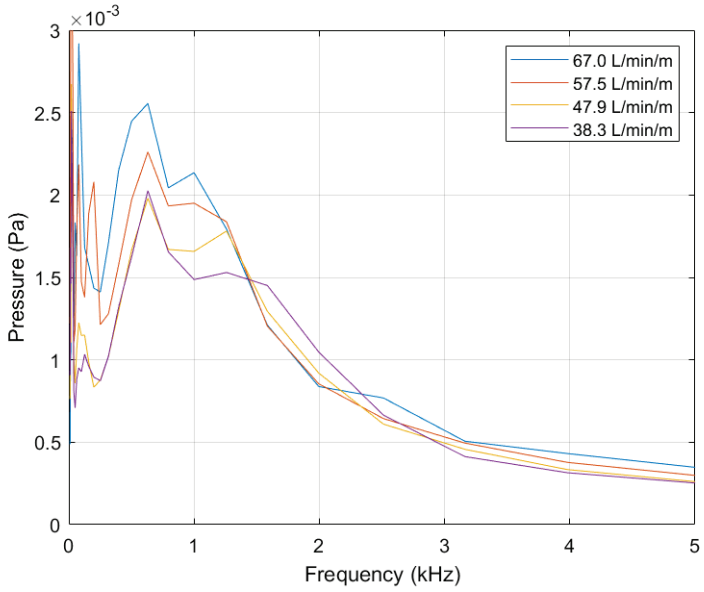

Figure 19 Two examples of bubble curtain noise taken using the SoundTrap at different flow rates. The SoundTrap was positioned approximately 60 cm away from the curtain.

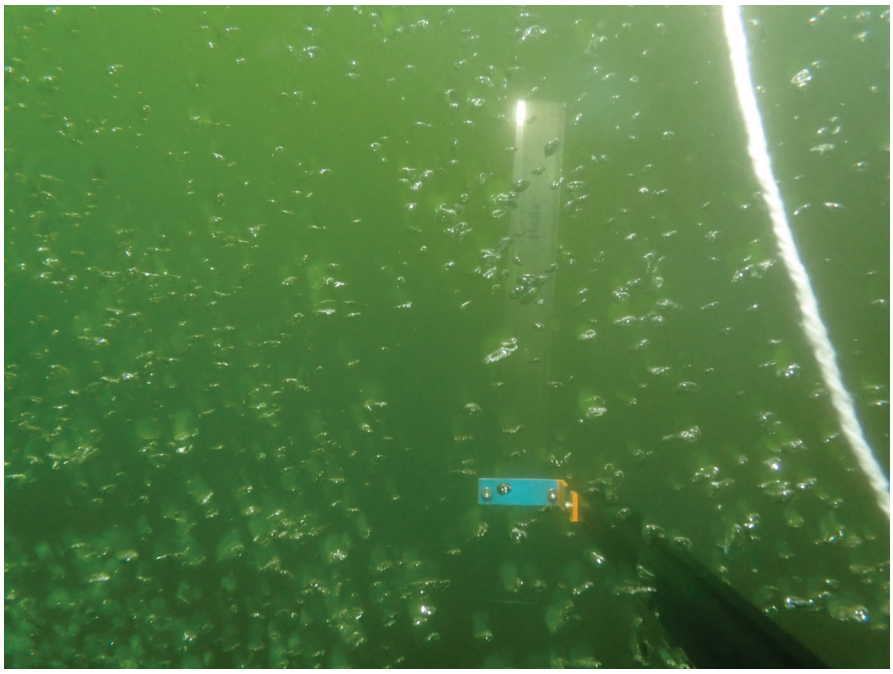

Figure 20 An example photograph of the bubble field at a flow rate of 67 L/min/m. For scale, the ruler is 30 cm long and the blue part of the mount is 5 cm long.

In Figure 18, the noise is centred around 100 Hz and 900 Hz, this corresponds to a bubble radius of 20 mm and 3.7 mm (using Minnaert's equation, (Leighton, 1994)). A bubble radius of 20 mm is highly unlikely and does not correlate to the bubbles that can be seen in Figure 20. However, 3.7 mm is more realistic and fits with the approximate bubble sizes shown in Figure 20. In Figure 19, it can be seen that the noise centred around 100 Hz has reduced in amplitude as the flow rate is reduced, the blue line being a second measurement of the bubble curtain noise at 67.0 L/min/m. At the lowest flow rate, the pressure level has reduced, or potentially spread out to cover a larger range of frequencies. This is an indication that the bubble field may cover a larger range of bubble sizes (smaller bubbles) and/or have fewer bubbles.

4 CONCLUSION

4.1 SUMMARY

A total of 23 shots were undertaken during a 6-day trial at the Limehillock Quarry test facility in order to assess the effects of a bubble curtain on the acoustic signal generated by explosions of similar sizes to those used in low-order deflagration.

Three different test regimes were conducted. Firstly, varying the charge size showed that increasing the charge size reduced the attenuation provided, this highlights the need to tailor the bubble curtain to the charge size required. Secondly, increasing the distance between the curtain and the charge increases the attenuation provided by the curtain up to around 3x the explosive bubble radius (at which point the curve levels off). This demonstrates that a larger radius of curtain is beneficial, although there will a practical trade off. Lastly, increasing the flow rate of the bubble curtain increased the attenuation provided. Limited data was collected with different curtain parameters (hole size, double/single curtain) so a full conclusion could not be formed. Attenuations were assessed for both L_{pk} and SEL metrics, where the highest attenuations were observed in the L_{pk} metric with the typical SEL attenuations achieved were around 4-5 dB lower. However, further experiments are required to understand these results fully.

Some measurements were carried out to investigate the bubble size produced by the curtains (~4 mm radius), these gave an indication of the bubble size but further tests are required to understand this and categorise the bubble size distribution fully.

4.2 DISCUSSION

This trial has provided a great deal of extra information around the parameters (summarised in the previous section) which may be useful to those using bubble curtains for mitigating the acoustic field generated by explosions. Direct comparison of signals from free field explosive sources were attenuated by the bubble curtains tested.

Similar to the last trial conducted by NPL in 2023 (Cheong et al., 2023) , there are some factors which should be considered when evaluating the results, such as the tightly controlled test environment providing less variation than an offshore deployment and the bubble curtain/charge being placed mid water column rather than on the floor (see 2023 report for further details).

4.3 FUTURE WORK

To fully explore the trends shown by the results in this report, it would be beneficial to undertake take further tests, particularly for the stand-off distance, to test larger distances between the charge and curtain, and also for the different bubble curtain parameters. The maximum flow rate that could be tested was limited by the compressor available at the site, so having a compressor capable of providing larger flow rates would increase the different bubble curtain parameters we could test (for example, multiple layers of curtains at higher flow rates).

References

Arons, A.B., (1954)., Underwater explosion shock wave parameters at large distances from the charge., *J. Acoust. Soc. Am.* 26, 343–346.

Arons, A.B., 1970. Evolution of explosion pressure - Wave Characteristics in the Region Relatively Close to the Origin

Beelen, S., Nijhof, M., de Jong, C., van Wijngaarden, L., & Krug, D. (2024). *Bubble curtains for noise mitigation: one vs. two*. http://arxiv.org/abs/2410.14415

Bohne, T., Grießmann, T., & Rolfes, R. (2019). Modeling the noise mitigation of a bubble curtain. *The Journal of the Acoustical Society of America*, *146*(4), 2212–2223. https://doi.org/10.1121/1.5126698

Cheong, S. H., Wang, L., Lepper, P., & Robinson, S. (2023). *Characterisation of acoustic fields generated by UXO removal phase 5 quarry trials of ESC low order technology*. https://doi.org/10.47120/npl.AC23

Cole, P., (1947), Underwater explosion. Princeton: Princeton University Press.

Croci, K., Arrigoni, M., & Jacques, N. (2014). *Mitigation of underwater explosion effects by bubble curtains : experiments and modelling*. http://sam.ensam.eu

Dam, T. T., & Tran, V. D. (2021). Research on the influence of bubble curtains on shock wave fields of the underwater explosion. *Journal of Mining and Earth Sciences*, *62*(5), 97–105. https://doi.org/10.46326/JMES.2021.62(5).09

Department for Environment, F. & R. A. (2025). *Marine environment: unexploded ordnance clearance Joint Position Statement*. https://www.gov.uk/government/publications/reducing-marine-noise/reducing-marine-noise#contents

Domenico, S. N. (1982). Acoustic wave propagation in air-bubble curtains in water-Part I: History and theory I PREVIOUS AND PRESENT APPLICATIONS. In *GEOPHYSICS* (Vol. 47, Issue 3). http://library.seg.org/

JNCC. (2010). *JNCC guidelines for minimising the risk of injury to marine mammals from using explosives*.

Leighton, T.G. (1994) The Acoustic Bubble. United Kingdom: Academic Press

Loye, D. P., & Fred Arndt, W. (1948). A Sheet of Air Bubbles as an Acoustic Screen for Underwater Noise. *Acoustical Society of America*, *20*.

National Marine Fisheries Service, U. S. D. of C. N. (2018). 2018 Revisions to: Technical guidance for assessing the effects of anthropogenic sound on marine mammal hearing (Version 2.0). . In *NOAA Technical Memorandum NMFS-OPR-59*.

National Marine Fisheries Service (2024). Update to: Technical Guidance for Assessing the Effects of Anthropogenic Sound on Marine Mammal Hearing (Version 3.0): Underwater and InAir Criteria for Onset of Auditory Injury and Temporary Threshold Shifts. U.S. Dept. of Commer., NOAA. NOAA Technical Memorandum NMFS-OPR-71, 182 p., https://www.fisheries.noaa.gov/resources/documents.

Robinson, S.P., Wang, L., Cheong, S-H., Lepper, P.A., Marubini, F. & Hartley, J.P., (2020), Underwater acoustic characterisation of unexploded ordnance disposal using deflagration, *Mar. Pollut. Bull.*, 160, Article 111646., https://doi.org/10.1016/j.marpolbul.2020.111646

Robinson, S.P. Wang, L., Cheong, S-H., Lepper, P.A., Hartley, J.P., Thompson, P.M., Edwards, E., & Bellmann, M., (2022), Acoustic characterisation of unexploded ordnance disposal in the North Sea using high order detonations, *Marine Pollution Bulletin, Vol. 184,* 114178, ISSN 0025-326X, https://doi.org/10.1016/j.marpolbul.2022.114178.

Schmidtke, E. (2010). *Shock wave attenuation with an air bubble curtain to protect marine mammals*. www.onlinedoctranslator.com

Schmidtke, E. (2012). *Shock wave attenuation with a veil of air bubbles in shallow water*. www.onlinedoctranslator.com

Sebastian Bryson, L., Smith, P. R., & Mahboub, K. C. (2021). A rational bubble screen design approach for mitigation of underwater explosion near waterborne infrastructure. *Canadian Journal of Civil Engineering*, *48*(3), 298–311. https://doi.org/10.1139/cjce-2019-0433

Southall, B. L., Bowles, A. E., Ellison, W. T., Finneran, J. J., Gentry, R. L., Greene, C. R., Kastak, D., Ketten, D. R., Miller, J. H., Nachtigall, P. E., Richardson, W. J., Thomas, J. A., & Tyack, P. L. (2007). Overview. *Aquatic Mammals*, *33*(4), 411–414. https://doi.org/10.1578/AM.33.4.2007.411

Urick, R.J. (1983) Principles of Underwater Sound. Connecticut:Peninsula Publishing.

Weston, D., (1960). Underwater explosions as acoustic sources. *Proc. Phys. Soc.* 76, 233–249.